Structural Chemistry (2018) 29:1341–1350
https://doi.org/10.1007/s11224-018-1119-z

ORIGINAL RESEARCH

Theoretical study on the substituent effect of halogen atom at different position of 7-azaindole-water derivatives: relative stability and excited-state proton-transfer mechanism

Jiacheng Yi[1] · Hua Fang[1]

Received: 20 October 2017 / Accepted: 24 April 2018 / Published online: 3 May 2018

Abstract
We have theoretically investigated the substituted effect on the first excited-state proton-transfer process of $nX7AI\text{-}H_2O$ ($n = 2\sim6$, X = F, Cl, Br) complex at the TD-M06-2X/6-31 + G(d, p) level. Here X is the substituted halogen atom, and n value denotes the substituted position of X, such as C_2, C_3, C_4, C_5, or C_6. For the substituted 7-azaindole clusters, $6X7AI\text{-}H_2O$ molecule is the most stable structure in water. The replacement of halogen atom X does not affect the characters of the HOMO and LUMO, but influence the $S_0 \rightarrow S_1$ adiabatic transition energies of $nX7AI\text{-}H_2O$ ($n = 2\sim6$, X = F, Cl, Br). Our calculated results show that the double proton transfer occurs in a concerted but asynchronous protolysis pathway no matter which H atom is replaced by halogen atom. The halogen substitution changes the structural parameters evidently and leads to amply the asynchronousity during the proton-transfer process. The ESPT barrier height increases or decreases due to the halogen atom and substituted position.

Keywords Excited-state · Proton transfer · Substituent effect · Concerted · Asynchronous

Introduction

Proton transfer is the most fundamental and important reactions because it is relevant to many chemical and biological processes [1–14]. Among all kinds of proton-transfer reactions, intermolecular excited-state proton transfer (ESPT) has been a hot topic and drawn much attention for decade years [15–17]. ESPT reactions took place in some family of compounds, in which the acidities were strengthened in the excited-state and known as photoacids [18]. In the ESPT process, photoacid transfers a proton from a proton donor (–OH or –NH group) to the proton acceptor (–C = O or –N = N group). A large number of biological phenomena such as DNA damage and some enzymatic reactions are caused by ESPT [19, 20]. Most proton-transfer reactions in proteins often occur along long-distance hydrogen-bonded (H-bonded) chain or network, such as polar amino acids or water molecules [7–11]. However, it is very hard to directly investigate such long-distance proton-transfer reaction along a proton wire experimentally and theoretically at the molecular level owing to the complicated structure and large mass protein [9, 11–13]. Hence, building a simplified model to simulate the biological proton-transfer process is very necessary.

Among many photoacid molecules, 7-azaindole (7AI) often serves as a model complex to research ESPT process since it resembles to DNA base pair [21] and has aroused much interest. 7AI has a proton donor (N–H) in the five-membered pyrrole ring and a proton acceptor (= N-) in the six-membered pyridine ring. An intermolecular H-bonded chain can be formed between N–H and = N- upon dimerization and complexation with polar solvents. 7AI occurs ESPT reaction along the H-bonded chain. Excited-state proton-transfer reactions in the 7AI dimer and 7AI-$(Solvent)_n$ clusters (Solvent: H_2O, CH_3OH, NH_3, etc.) [22–41] have been widely studied experimentally and theoretically. Many theoretical results showed that ESPT in the 7AI-$(Solvent)_n$ complexes in gas happened in the concerted but asynchronous pathway [25, 36, 38, 40, 41]. Yu et al. [42, 43] found that the ESPT

Electronic supplementary material The online version of this article (https://doi.org/10.1007/s11224-018-1119-z) contains supplementary material, which is available to authorized users.

✉ Hua Fang
susanfang20@gmail.com

[1] Department of Chemistry and Material Science, College of Science, Nanjing Forestry University, Nanjing 210037, People's Republic of China

processes in the 7AI dimer and (3-methyl-7AI)-7AI complex preferred the concerted but asynchronous mechanism by using the multireference second-order perturbation theory (CASPT2) and time-dependent density functional theory (TDDFT) with long-range correction. Sakota et al. [31, 37] researched the excited-state proton-transfer reactions in 7AI–$(H_2O)_2$ and 7AI–$(CH_3OH)_2$ complexes experimentally and concluded that triple protons transferred asynchronously but concertedly. They also observed the vibration-mode-specific nature of ESPT. The nature of vibration-mode-specific was reproduced theoretically [40]. Theoretical results indicated that the vibrational-mode selectivity can effectively shorten the ESPT path and accelerate the rate of ESPT.

Detailed investigations on ESPT were focused on understanding the tautomerization dynamics and abstracting useful information related to mechanism in order to regulate proton-transfer process [24, 25, 27, 33, 44]. The dynamics and thermodynamics of ESPT correlate with the kinetics of proton motion and H-bonding strength, namely proton donating (acidity) and accepting (basicity) abilities. Chemical modification by a substituent group R can regulate the H-bonding strength depending on the electronic nature of R. Krygowski et al. [45] studied the substituent effect on proton transfer in para-substituted phenol complexes with seven substituents (-NO, $-NO_2$, -CHO, -H, $-CH_3$, $-OCH_3$, -OH) at the B3LYP/6–31++G(d, p) level. They concluded that the H-bonding strength and the position of proton transfer linearly correlated to the Hammett substituent constants. Chou et al. [46] researched the excited-state proton-transfer process in the 3-cyano-7-azaindole complex, in which the cyano substituted H atom of C_3 position in pyrrole ring. They found that the acidity of N–H group in the 3-cyano-7-azaindole complex was increased, and the ESPT rate in water was speeded up due to the electron-withdrawing ability of the cyano group. Tseng et al. [47] investigated excited-state intramolecular proton transfer (ESIPT) in many N-H type H-bonding complexes, in which one of the amino hydrogens was replaced with electron-donating/withdrawing groups. They concluded that the H-bonding strength affected the ESIPT dynamics and thermodynamics. The larger electron-withdrawing ability of the substituent increased the acidity of the NR–H proton, strengthened the H-bond, and quickened ESIPT process. Very recently, Chen et al. [48] studied series of N–H seven-membered-ring H-bonded molecules and confirmed that the strong H-bond was advantageous to ESIPT process thermally.

Substituent effect is also relevant to the position of substituent group, and it is named steric effect. Nazarparvar et al. [49] investigated the substituent effects on the O–H bond dissociation enthalpies (BDEs) of trans-resveratrol derivatives, in which electron-donating and -withdrawing groups were placed in four positions. They found that the BDEs were affected by the mutual positions of substituents and OH groups. Klein et al. [50] studied the reaction enthalpies of the individual steps of two antioxidants action mechanisms in meta- and para-substituted phenols. They found that electron-donating substituents increased the enthalpies of proton dissociation and proton affinity. Electron-withdrawing groups increased the reaction enthalpies of the reactions where electron was abstracted. The reaction enthalpies linearly correlated with Hammett constants of the substituents. And the substituents in meta- position had a great effect on ionization potential and enthalpy of proton dissociation. Solntsev et al. [51] carried out a study on the excited-state dynamics of the meta- and para- isomers of the green fluorescent protein chromophore and its O-methylated derivative. They observed the first excited-state was fast quenched to the ground state by internal conversion in all compounds. Internal conversion may promote by the internal twisting in the para compounds. A similar process emerged slowly in the meta compounds but with obviously slower kinetics. The meta compounds can occur ultrafast intermolecular excited-state proton transfer in aqueous.

It is obvious that substituent group and the position of the substituent can effectively control the kinetics and thermodynamics of ESPT. Thus, we used a cyclic H-bonded complex having been chemically modified with substituent at different positions as a simple model to study the excited-state tautomerization process.

In this work, we presented a detailed study on the excited-state proton-transfer process in the 7AI–H_2O derivatives nX7AI–H_2O ($n = 2\sim6$; X = F, Cl, Br) (see Fig. 1),

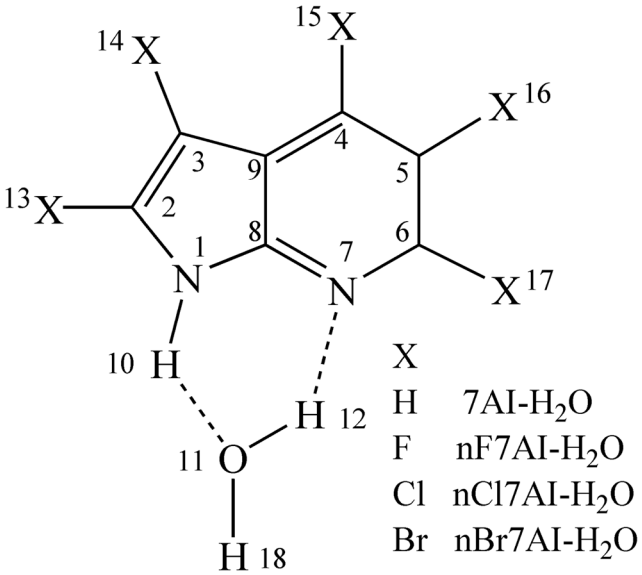

Fig. 1 Molecular structure of the 7AI–H_2O complex and its derivatives (denoted as nX7AI–H_2O ($n = 2\sim6$; X = F, Cl, Br); n value denotes the substituted position

in which the hydrogen atoms at C_2, C_3 position in pyrrole ring near N–H···O, and C_4, C_5, C_6 position in pyridine ring near N···H H–Bond were replaced by halogen atom X (X = F, Cl, Br). We aimed to investigate the role of the substituent group and different substituent position to the relative stability of nX7AI–H_2O and the ESPT thermodynamics and kinetics.

Computational details

All the structures of the reactant, product, and transition state (TS) in the first excited-state (S_1) tautomerization in the 7AI–H_2O derivatives were fully optimized in solution with TD-M06-2X [52] method and 6-31 + G(d, p) basis set using Gaussian 09 program [53]. The optimized ground state geometries of 7AI–H_2O and its derivatives were obtained at the M06-2X [52]/6-31 + G(d, p) level. 7AI–H_2O derivatives are the molecules that the H atoms at C_2, C_3 position in pyrrole ring near N-H···O H-bond, and C_4, C_5, C_6 position in pyridine ring near N···H H-bond in the 7AI–H_2O complex were replaced by halogen atom X (X = F, Cl, Br) and denoted as nX7AI–H_2O (n = 2~6, X = F, Cl, Br). The vibrational frequencies were also calculated at the TD-M06-2X/6-31 + G(d, p) level in order to confirm the optimized equilibrium structures were minima (reactant and product) and transition state on the potential energy surface. The optimized reactant/product and transition state had no imaginary frequency and only one imaginary frequency, respectively. M06-2X functional is the suitable method to research main-group themochemistry, thermochemical kinetics, noncovalent interactions, and excited-states [52]. In order to consider the solvent effect, the integral equation formalism polarizable continuum model (IEFPCM) [54–56] was used. The atomic radii from the UFF force field were scaled by 1.1 in the IEFPCM model. In the solution calculation, water with a dielectric constant of 78.3 was chosen as solvent. To investigate the chemical bond in 7AI-H_2O derivatives, the natural bonding orbital (NBO) analysis [57–59] was applied to the optimized structure at the same computational level.

Results and discussion

Relative stability of nX7AI–H_2O (n = 2~6, X = F, Cl, Br) complex

The relative energies ΔE and Gibbs free energies ΔG of nX7AI–H_2O (n = 2~6; X = F, Cl, Br) complexes are presented in Table 1. The Gibbs free energies were computed at the 298.15 K under 1 atm. Among the isomers of nX7AI–H_2O (n = 2~6; X = F, Cl, Br) complexes, 6X7AI–H_2O molecule is the most stable one in water. The results in Table 1 indicated that different halogen substitution had different order of the relative stabilities of these isomers. For F-substitutions, the relative stabilized trend is 6F7AI–H_2O > 5F7AI-H_2O > 3F7AI–H_2O > 4F7AI–H_2O > 2F7AI–H_2O. When the substituted atom X is Cl and Br, the trend of relative stabilities of nX7AI–H_2O isomers is 6X7AI–H_2O > 4X7AI–H_2O > 3X7AI–H_2O > 2X7AI–H_2O > 5X7AI–H_2O. Table 2 listed the Boltzmann population ratios of nX7AI–H_2O which were calculated with the IEFPCM model at 298.15 K and 1 atm. As shown in Table 2, among F-, Cl-, or Br-substitutions, the 6X7AI-H_2O complex is the main existing form in water.

Frontier molecular orbitals

The dynamics of the first excited-state tautomerization in the heteroaromatic molecules and their H-bonded clusters are determined by the relative energetics of the $S_{\pi\pi^*}$ and $S_{\pi\sigma^*}$ states. The ESPT reaction occurs on the ππ* state, and the excited-state hydrogen-atom transfer (ESHT) reaction may occur through πσ* state [60–63]. In order to understand the nature of the excited-state tautomerization in the nX7AI–H_2O (n = 2~6, X = F, Cl, Br) complexes, we analyzed the highest occupied molecular orbital (HOMO) and the lowest unoccupied molecular orbital (LUMO) which was obtained at the TD-M06-2X/6-31 + G(d, p) level. The 7AI–H_2O complex serves as an example of all complexes, and the HOMO and LUMO of 7AI–H_2O are displayed in Fig. 2 (MOs of other complexes nX7AI–H_2O (n = 2~6, X = F, Cl, Br) are depicted in Fig. S1).

By comparing the shapes of HOMO and LUMO, nX7AI–H_2O (n = 2~6, X = F, Cl, Br) is an obvious ππ*-type transition. The character of the π → π* transition is the exact proof for

Table 1 Relative energies (ΔE, kcal/mol) and Gibbs free energies (ΔG, kcal/mol) of 7AI–H_2O and nX7AI–H_2O (n = 2~6; X = F, Cl, Br) complexes in water

Species	Parameter	6X7AI–H_2O	5X7AI–H_2O	3X7AI–H_2O	4X7AI–H_2O	2X7AI–H_2O
X = F	ΔE	0	5.08	6.86	8.57	11.5
	ΔG	0	4.80	7.17	8.65	10.2
X = Cl	ΔE	0	8.39	2.16	1.75	7.49
	ΔG	0	7.31	2.38	1.90	6.38
X = Br	ΔE	0	7.60	1.35	0.22	6.84
	ΔG	0	6.87	1.80	1.00	6.51

Table 2 Boltzmann population ratios (%) of nX7AI–H_2O (n = 2~6; X = F, Cl, Br) complexes in water at 298.15 K and 1 atm

Species	X = F	X = Cl	X = Br
6X7AI–H_2O	100.00	94.48	81.13
5X7AI–H_2O	0.00	0.00	0.00
3X7AI–H_2O	0.00	1.70	3.88
4X7AI–H_2O	0.00	3.82	14.99
2X7AI–H_2O	0.00	0.00	0.00

proton-transfer reaction. The electron densities of both the HOMO and LUMO completely locate on the 7AI moieties, and no electron density localizes on water, so the H-bonded chain of water still remains in its electronic ground-state during the proton-transfer process. As shown in Fig. 2 and Fig. S1, the substituent halogen atom X at different positions had no effect on the characters of the HOMO and LUMO of nX7AI–H_2O complex.

The $S_0 \rightarrow S_1$ adiabatic transition energies of 7AI-H_2O and its derivatives nX7AI–H_2O (n = 2~6; X = F, Cl, Br) have been calculated on the optimized structures in the ground-state and first excited-state. The electronic excitation energies and the corresponding orbital transition contributions were listed in Table 3. The S_1 ($\pi\pi^*$) band origin of 7AI–H_2O has been reported experimentally by Hara et al. to 33,340 cm^{-1} (4.134 eV) [30]. The calculated adiabatic transition energy of 7AI–H_2O at the TD-M06-2X/6-31 + G(d,p) level amounts to 4.306 eV, which is comparable with experimental value with a deviation of + 0.157 eV. Our theoretical results of nX7AI-H_2O complexes based on TD-M06-2X/6-31 + G(d,p) level are reliable. As shown in Table 3, the electronic transition energies of nX7AI-H_2O complexes varied with the substituent X and substituted position.

The mechanism of excited-state proton transfer

The structures of stationary points in the cyclic nX7AI-H_2O (n = 2~6, X = F, Cl, Br) complexes were fully optimized in water at TD-M06-2X/6-31 + G(d, p) level. Some geometrical parameters of TS are listed in Table 4, and the structures of TS are displayed in Fig. S2. No matter which H atom at the C_2, C_3, C_4, C_5, or C_6 position of 7AI-H_2O complex was substituted for halogen atom X (X = F, Cl, Br), only one concerted but asynchronous TS was obtained without any intermediate for the excited-state double proton-transfer process in the nX7AI-H_2O (n = 2~6, X = F, Cl, Br) complexes. As shown in Table 4, N_1–H_{10}, H_{10}–O_{11}, O_{11}–H_{12}, and H_{12}–N_7 distances in TS of nX7AI-H_2O (n = 2~6, X = F, Cl, Br) are in the range of 1.279~1.383, 1.137~1.217, 1.070~1.105, and 1.446~1.523 Å, respectively. It is obvious that N_1–H_{10} distance is averagely 0.128 and 0.223 Å longer than H_{10}–O_{11} and O_{11}–H_{12} distances, respectively. These results indicated that H_{10} proton moves first and transfers more than halfway from N_1 to O_{11}, subsequently H_{12} proton moves a little from O_{11} to N_7, and a H_3O^+-like portion forms at O_{11}. The ESPT reaction in nX7AI-H_2O (n = 2~6, X = F, Cl, Br) complex occurred in a concerted but asynchronous protolysis [65] pattern. The concerted but asynchronous protolysis mechanism of ESPT was verified by NBO charges of the H_3O^+-like moiety of TS, which were listed in Table S1.

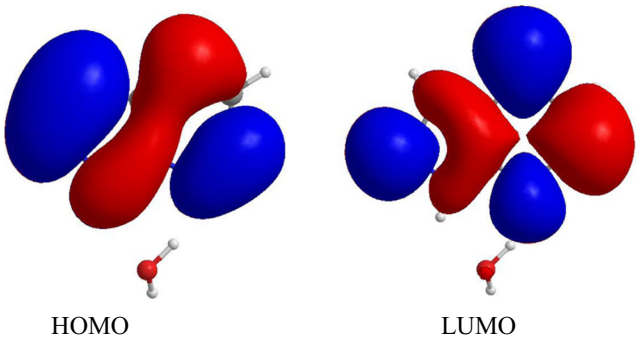

Fig. 2 The frontier molecular orbitals of 7AI–H_2O complex in the first excited-state (S_1) at the TD-M06-2X/6-31 + g(d, p) level

The character of TS during the proton-transfer process can be depicted in a correlation plot between the proton transfer coordinate and the H-bond distance. In A–H…B complex, the r_{AH} and r_{BH} distances conform to the Pauling equations and interrelate with each other, with the hypothesis that the sum of bond orders is conserved during proton-transfer process [66]. Limbach et al. [67–69] proposed to combine proton transfer and H-bonding distance in a correlation. The relationship between r_{AH} and r_{BH} in A–H…B complex can be expressed by H-bond coordinates $q_1 = {}^1/_2(r_{AH} - r_{BH})$ and $q_2 = r_{AH} + r_{BH}$. For a linear H-bond, q_1 represents the distance from H to the H-bonding center, and q_2 represents the distance between two heavy atoms A and B. The property of TS such as bond order, earliness or lateness, and synchronicity during proton-transfer process can be described in this correlation plot. When H moves from A to B in the A–H···B complex, q_1 value varies from negative to positive, and q_2 situates at $q_1 = 0$ after passing through a minimum. There is a correspondence between late/early TS and positive/negative q_1 value. And a tight or loose TS corresponds to a small or big q_2 value, respectively. When several protons relay in the synchronous or asynchronous mechanism, the multiple q_1 values of TS should be alike or different to each other, respectively.

The correlations between N_1–H_{10} and H_{10}–O_{11} distances (H_{10} transfer), and O_{11}–H_{12} and H_{12}–N_7 distances (H_{12} transfer) in the TS are depicted in Fig. 3. The correlation points of the TS in the nX7AI-H_2O (n = 2~6; X = F, Cl, Br) complexes are all at or close to the black line according to Pauling equation, which means that the bond orders are conversed. For the nX7AI-H_2O (n = 2~6; X = F, Cl, Br) complexes, the q_1 values of H_{10} transfer at the TS are near zero or slightly positive, which represents that H_{10} is nearly in the center between N_1

Table 3 Electronic excitation energy (eV) of $S_0 \rightarrow S_1$, oscillator strengths, and the corresponding orbital transition contributions for nX7AI-H_2O (n = 2~6; X = H, F, Cl, Br) in water

Complex	Electronic excitation energy	Oscillator strengths	Orbital contributions
7AI-H_2O[a]	4.134		
7AI-H_2O	4.306	0.267	HOMO→LUMO 98.4%
2F7AI-H_2O	4.439	0.2884	HOMO→LUMO 98.4%
2Cl7AI-H_2O	4.358	0.4108	HOMO→LUMO 98.4%
2Br7AI-H_2O	4.326	0.4751	HOMO→LUMO 98.2%
3F7AI-H_2O	4.111	0.2114	HOMO→LUMO 98.4%
3Cl7AI-H_2O	4.159	0.2003	HOMO→LUMO 98.4%
3Br7AI-H_2O	4.161	0.1942	HOMO→LUMO 98.4%
4F7AI-H_2O	4.497	0.2233	HOMO→LUMO 98.3%
4Cl7AI-H_2O	4.268	0.2762	HOMO→LUMO 98.3%
4Br7AI-H_2O	4.227	0.3341	HOMO→LUMO 98.1%
5F7AI-H_2O	4.215	0.2477	HOMO→LUMO 98.2%
5Cl7AI-H_2O	4.468	0.2239	HOMO→LUMO 95.6%
5Br7AI-H_2O	4.430	0.2303	HOMO→LUMO 95.4%
6F7AI-H_2O	4.310	0.2132	HOMO→LUMO 98.7%
6Cl7AI-H_2O	4.224	0.2655	HOMO→LUMO 98.4%
6Br7AI-H_2O	4.196	0.2906	HOMO→LUMO 98.2%

[a] The experimental value for S_1 0–0 band of 7AI-H_2O has been adopted from ref. [30]

and O_{11}. At the same time, the H_{12} correlation points emerge in the upper-left area; the q_1 values of H_{12} transfer at the TS are very negative, which represent that H_{12} is close to O_{11}. The correlation plot indicated that the double-proton transfer in the nX7AI-H_2O complexes occurred in a concerted but highly asynchronous mechanism (a little late TS for H_{10} but very early for H_{12} transfers) and generated a $[H_3O]^+$-like portion as part of TS.

Table 4 Geometric parameters (Å) of transition states for excited-state proton transfer in 7AI-H_2O and nX7AI-H_2O (n = 2~6; X = F, Cl, Br) complexes in water

	Transition state			
System	r(N_1-H_{10})	r(H_{10}-O_{11})	r(O_{11}-H_{12})	r(H_{12}-N_7)
7AI-H_2O[a]	1.287	1.215	1.126	1.410
2F7AI-H_2O[a]	1.279	1.217	1.070	1.523
2Cl7AI-H_2O[a]	1.293	1.206	1.082	1.496
2Br7AI-H_2O[a]	1.297	1.202	1.086	1.486
3F7AI-H_2O	1.293	1.208	1.101	1.452
3Cl7AI-H_2O	1.297	1.205	1.101	1.454
3Br7AI-H_2O	1.293	1.208	1.104	1.447
4F7AI-H_2O	1.315	1.189	1.100	1.455
4Cl7AI-H_2O	1.312	1.192	1.105	1.446
4Br7AI-H_2O	1.314	1.191	1.104	1.448
5F7AI-H_2O	1.311	1.192	1.102	1.449
5Cl7AI-H_2O	1.320	1.185	1.096	1.462
5Br7AI-H_2O	1.320	1.184	1.095	1.464
6F7AI-H_2O	1.383	1.137	1.083	1.485
6Cl7AI-H_2O	1.359	1.153	1.086	1.479
6Br7AI-H_2O	1.361	1.152	1.088	1.477

[a] Ref [64]

The energetics of excited-state proton transfer

The excited-state double proton relay reaction energies (ΔE) and the barrier heights (ΔV) in the nX7AI-H_2O (n = 2~6; X = F, Cl, Br) complexes were shown in Table 5. The reaction energies without and with zero-point energy (ZPE) corrections of nX7AI-H_2O complexes are in the range of − 5.98~− 19.7 kcal/mol and − 5.96~− 18.8 kcal/mol, respectively. The ESDPT reactions in the nX7AI-H_2O complexes are exothermic. The TS structure of nX7AI-H_2O would be similar to the reactant. With and without ZPE-corrected barrier heights of ESDPT in the nX7AI-H_2O complex are in the range of 1.99~9.30 and 4.43~12.4 kcal/mol, respectively. It is evident that the barrier height of ESDPT is dependent on the substituent halogen atom and substituted position.

Substituent effect

In order to investigate the effect of halogen substitution at the different positions of 7AI-H_2O complex, we compared the results of ESDPT in the nX7AI-H_2O (n = 2~6; X = F, Cl, Br) complexes to those of 7AI-H_2O [64] and found some resemblances and differences. The nature of ESPT in the nX7AI-H_2O (n = 2~6; X = F, Cl, Br) complex is the $\pi \rightarrow \pi^*$ transition no matter which halogen atom X substituted for H atom at

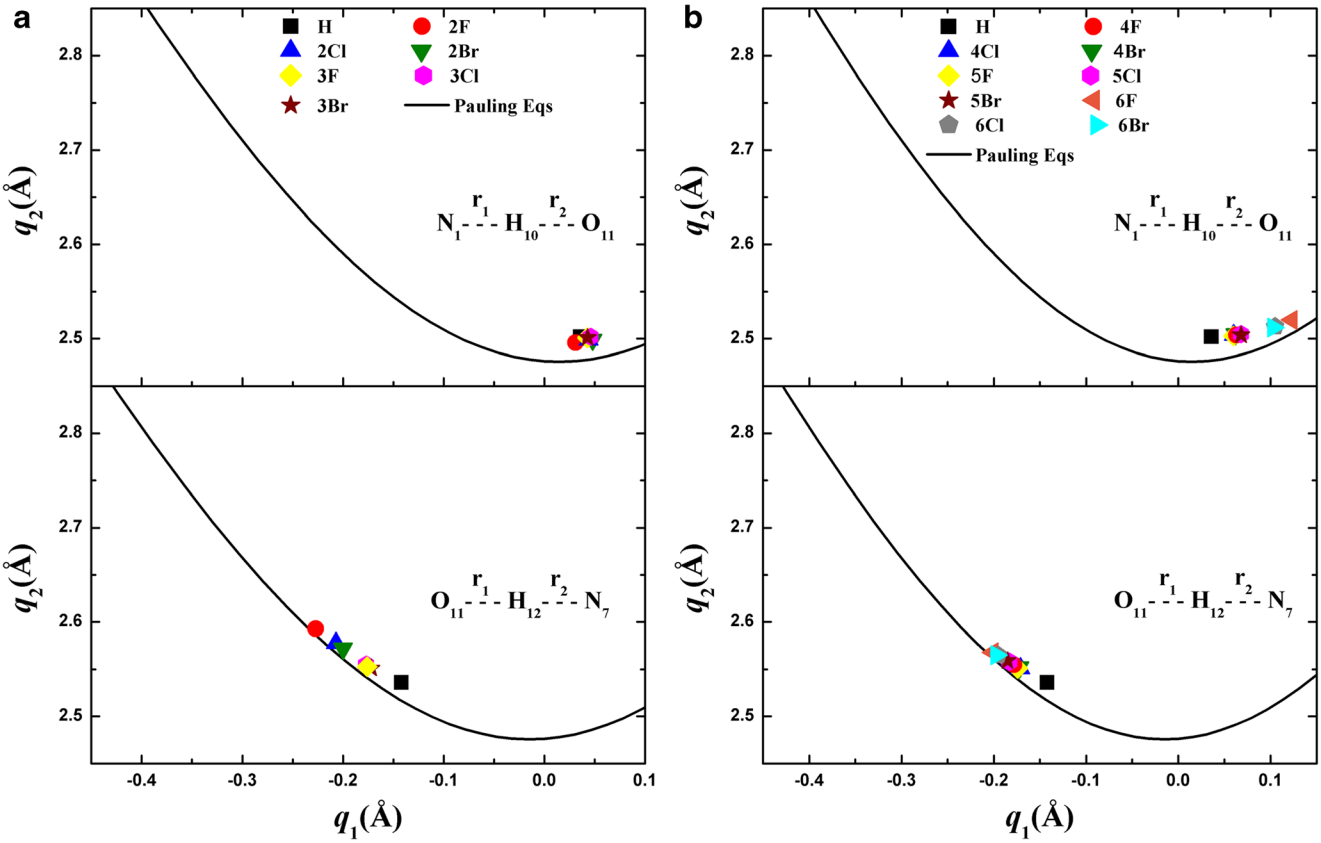

Fig. 3 Correlation of the H-bond distances, $q_2 = r_1 + r_2$, with the proton transfer coordinate, $q_1 = 1/2(r_1\text{-}r_2)$, for the 7AI-$H_2O$ and nX7AI-H_2O ($n = 2$~6; X = F, Cl, Br) complexes in water. Top, H_{10} transfer; bottom, H_{12} transfer. All points are for the transition state in S_1 optimized at the TD-M06-2X/6-31 + G(d, p) level. The solid lines designate the correlation that satisfies conservation of the bond order. The parameters for Pauling equations were from the literature [67]. The correlation points of 7AI-H_2O complex are from the literature [64]. The regions above and below the black line are where the sums of bond orders are smaller and larger than unity, respectively

C_2~C_6 position in 7AI-H_2O complex. The excited-state proton transfer in the 7AI-H_2O complex occurred via a highly asynchronous but concerted protolysis pathway. The nX7AI-H_2O ($n = 2$~6; X = F, Cl, Br) complexes originate from 7AI-H_2O complex by replacing H atom at different position (C_2, C_3, C_4, C_5 or C_6) in the pyrrole and pyridine ring in the 7AI-H_2O complex with halogen atom X (X = F, Cl, Br). The substituted halogen atom X did not influence the ESDPT mechanism. The

Table 5 Reaction energies (ΔE) and barrier heights (ΔV) for excited-state proton transfer in nX7AI-H_2O ($n = 2$~6; X = H, F, Cl, Br) complexes in water

Species	ΔV				ΔE			
	X = H[a]	X = F	X = Cl	X = Br	X = H[a]	X = F	X = Cl	X = Br
2X7AI-H_2O[a]	10.6 (6.86)	7.35 (4.62)	8.82 (5.75)	9.25 (6.14)	− 13.6 (− 13.2)	− 19.7 (− 18.8)	− 17.0 (− 16.5)	− 16.1 (− 15.7)
3X7AI-H_2O	10.6 (6.86)	9.19 (5.77)	9.29 (6.13)	9.40 (5.96)	− 13.6 (− 13.2)	− 15.3 (− 15.0)	− 15.4 (− 15.0)	− 15.3 (− 15.0)
4X7AI-H_2O	10.6 (6.86)	10.9 (7.46)	10.8 (7.20)	10.8 (7.45)	− 13.6 (− 13.2)	− 12.8 (− 13.4)	− 12.5 (− 12.5)	− 12.3 (− 11.9)
5X7AI-H_2O	10.6 (6.86)	10.5 (7.13)	4.43 (1.99)	5.04 (2.37)	− 13.6 (− 13.2)	− 12.7 (− 12.2)	− 18.3 (− 17.2)	− 17.6 (− 16.7)
6X7AI-H_2O	10.6 (6.86)	12.4 (9.30)	11.9 (8.78)	11.9 (8.80)	− 13.6 (− 13.2)	− 5.98 (− 5.96)	− 7.98 (− 7.80)	− 7.98 (− 7.70)

The numbers in parentheses include zero-point energies. Energies are in kcal/mol

[a] Values come from Ref [64]

excited-state proton transfer in the *nX*7AI-H_2O complexes still preferred a concerted but asynchronous protolysis path. Besides, there are some differences in ESPT process in the *nX*7AI-H_2O complexes.

Firstly, the $S_0 \rightarrow S_1$ adiabatic transition energies of 7AI-H_2O and its derivatives *nX*7AI-H_2O ($n = 2$~6; X = F, Cl, Br) changed with substituted halogen atom X and position. When the H atom at C_2 and C_3 positions in the 7AI-H_2O complex are substituted for halogen atom X (X = F, Cl, Br), the transition energy averagely increases 0.070 eV and decreases 0.162 eV, respectively, comparing to that value in the 7AI-H_2O complex. When the substituted position is C_4 and C_6, F-, and Cl-, Br-substituted complexes have larger and smaller transition energy than 7AI-H_2O complex, respectively. When the substituted position is C_5, the transition energy of 5F7AI-H_2O increases, whereas the transition energies of 5Cl7AI-H_2O and 5Br7AI-H_2O decrease. The transition energies in the *nX*7AI-H_2O (X = F, Cl, Br) complexes are linearly dependent on the Pauling electronegativity of halogen atom X (see Fig. S3).

Secondly, halogen atom X as the substituent affected the H-bond distances of reactant and product in the *nX*7AI-H_2O (n = 2~6; X = F, Cl, Br) complexes obviously. The structural parameters of reactant and product in the *nX*7AI-H_2O ($n = 2$~6; X = F, Cl, Br) complexes were listed in Table S2, and the changes of the H-bond distances were discussed in detail in Supporting Information. The H-bond length is shorter; the H-bond energy is higher, and the proton transfers easier. This is a common rule for a single H-bond. However, estimating the bond energy of a certain H-bond in a relay chain is very difficult. Hence, it is necessary to verify that the common regularity between H-bond distance and energy is applicable to the H-bonded relay chain by using NBO analysis of H-bond [57–59]. As an important part of the H-bond, the charge transfer between the lone pair electron of N/O and anti-bonding orbital of N–H/O–H bond can be used to reckon the strength of H-bond. In NBO analysis, the charge-transfer energy infers donor-acceptor (bond-antibond) interactions. The larger the interaction energy of charge transfer, the stronger the H-bond. The H-bond distance and charge-transfer energies of each H-bond in the relay chain were listed in Table S3. We found that between the charge-transfer energy of each H-bond and its length has a good correlation (see Fig. 4), which means that the H-bond strengthens when the H-bond distance shortens. The bonds between the N–H bond and the acceptor O or N atom affected the proton-transfer process obviously [61, 70]. If the distance between two heavy atoms was too far, the barrier height of proton-transfer process was also too large since H-bond compression reduced the barrier height [71]. Namely, the distance between two neighboring end atoms of proton transfer in reactant such as N_1–O_{11} (R_1) and O_{11}–N_7 (R_2) plays a significant part in the tautomerization barrier. The

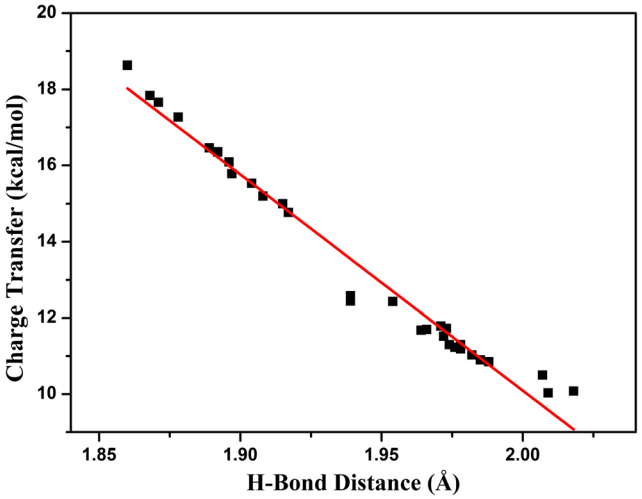

Fig. 4 Correlation between the H-bond distance and the charge transfer energy of the H-bonded chain in the 7AI-H_2O and *nX*7AI-H_2O ($n = 2$~6; X = F, Cl, Br) complexes

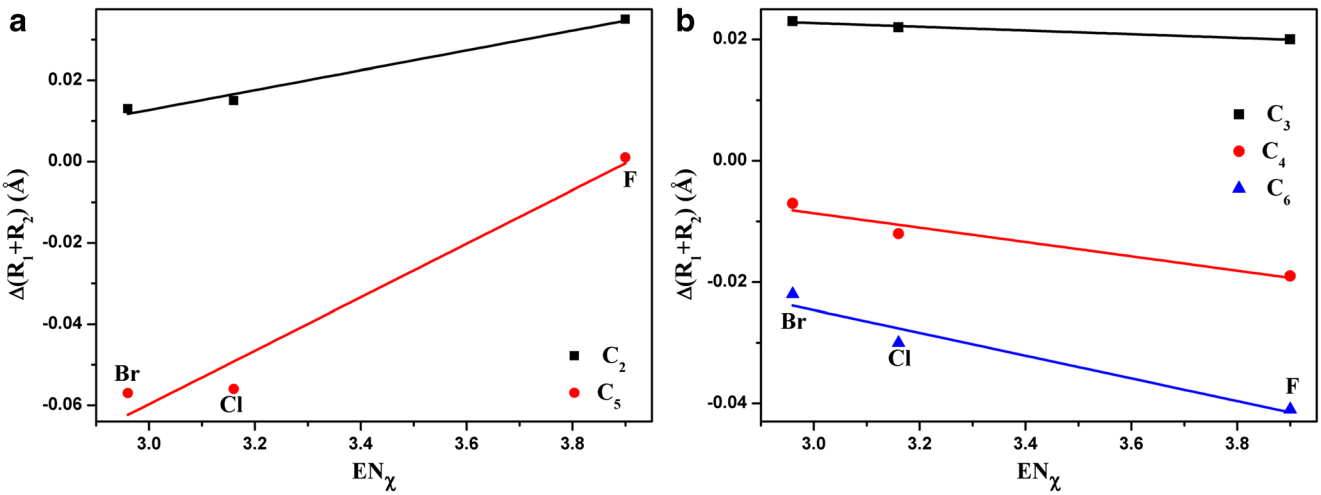

Fig. 5 Correlation between the change in the sum of the N_1–O_{11} (R_1) and O_{11}–N_7 (R_2) distances ($\Delta(R_1 + R_2)$) in the *nX*7AI-H_2O ($n = 2$~6; X = F, Cl, Br) complexes and the Pauling electronegativity (EN_χ) of X. **a** Substituted position C_2 and C_5. **b** Substituted position C_3, C_4, and C_6

distances of N_1–O_{11} (R_1) and O_{11}–N_7 (R_2) were listed in Table S1. In this work, $\Delta(R_1 + R_2)$ is used to represent the difference between the sum of the N_1–O_{11} and O_{11}–N_7 distances of nX7AI-H_2O and those values of 7AI-H_2O. We found that $\Delta(R_1 + R_2)$ and Pauling electronegativity of halogen atom X have good linear correlation (see Fig. 5). When the substituted position is C_2 and C_5, $\Delta(R_1 + R_2)$ increases with the decrescent Pauling electronegativity of X. When the substituted position is C_3, C_4, and C_6, $\Delta(R_1 + R_2)$ increases with the incremental Pauling electronegativity of X.

Thirdly, the structural parameters (see Table 4) in TS of nX7AI-H_2O (n = 2~6; X = F, Cl, Br) complexes also changed with the substituted halogen atom X and substituted positions. After the replacement of halogen atom at C_2 and C_3 positions, the N_1–H_{10} and H_{10}–O_{11} distances are a little shorter and longer than those distances in the nX7AI-H_2O (n = 4~6) complexes. Comparing to the structural parameters of TS in the 7AI-H_2O, the halogen substitutions make the N_1–H_{10}, H_{12}–N_7 and H_{10}–O_{11}, O_{11}–H_{12} distances of nX7AI-H_2O (except 2F7AI-H_2O) increase 0.030 Å, 0.054 Å and decrease 0.029 Å, 0.035 Å on average, respectively. In the 2F7AI-H_2O complex, the N_1-H_{10}, O_{11}-H_{12}, and H_{10}–O_{11}, H_{12}–N_7 distances reduced by 0.008 and 0.056 Å and increased by 0.002 and 0.113 Å, respectively.

A few differences appearing in the correlation plot were caused by these small changes on the structures. As shown in Fig. 3a, the H_{10} and H_{12} correlation points for TS in the 2X7AI-H_2O and 3X7AI-H_2O (X = F, Cl, Br) complexes are unchanged and move a little to the upper-left side along the black line, respectively, with the comparison to the corresponding points in the 7AI-H_2O. The locations of the TS on the H_{10} and H_{12} transfer are invariant and a bit late, respectively. When the halogen substitution is at C_4, C_5, and C_6 positions, the corresponding H_{10} and H_{12} points move a bit to the upper-right and upper-left sides along the Pauling line (see Fig. 3b), respectively. As a result, positions of the TS on the H_{10} and H_{12} transfer reaction coordinate in the nX7AI-H_2O (n = 4~6) complex are a little early and late, respectively. These results indicate that no matter which position in the 7AI-H_2O complex is substituted, the asynchronicity of proton transfer is enlarged evidently. The structural changes of the TS are possibly due to the electron-withdrawing ability of halogen atom X, which increases the acidity of N–H group of nX7AI-H_2O. The NBO charges of the H_3O^+-like portion in TS for the nX7AI-H_2O complex were in Table S1, and those values for the nX7AI-H_2O complex added 0.040 on average with comparison to that value for the 7AI-H_2O.

Lastly, the substituent halogen atom and substituent position in the 7AI-H_2O complex influenced the barrier height of ESDPT evidently. When the H atom at C_2 and C_3 position in the pyrrole ring was substituted by halogen atom X, the ZPE-corrected barrier height is in the range of 4.62~6.14 kcal/mol, which is 0.72~2.24 kcal/mol lower than that value of 7AI-H_2O complex. If the H atom at C_4 and C_6 position in the pyridine ring was replaced by halogen atom X, the ESDPT barrier height with ZPE-correction is in the range of 7.20~9.30 kcal/mol. The halogen replacements at C_4 and C_6 position increase the barrier height of ESDPT by 0.34~2.44 kcal/mol. And the replacement of X at C_5 position makes the barrier height rise/reduce due to the substituent halogen atom X. F-substitution increases the barrier height by 0.27 kcal/mol, while Cl- and Br-substitution decreases the barrier height by 4.87 and 4.49 kcal/mol, respectively.

Conclusions

In conclusion, a careful and detailed theoretical study on the halogen substituent effect upon the excited-state tautomerization process in the 7AI-H_2O complex in water were carried out at the TD-M06-2X/6-31 + G(d, p) level. The character of the $\pi \rightarrow \pi^*$ transition during the tautomerization process could be clearly seen, which could be the exact proof for proton-transfer reaction. For the nX7AI-H_2O (n = 2~6; X = F, Cl, Br) complexes, the ESPT reaction preferred a concerted but asynchronous protolysis pathway regardless of halogen atom or substituent position. In this path, H_{10} proton started the ESPT process and moved more than halfway from N_1 to O_{11}; H_{12} moved a little from O_{11} to N_7, and a H_3O^+-like portion generated at O_{11}.

The halogen substitution at C_2, C_3, C_4, C_5, and C_6 positions had little effect on the mechanism and the nature of ESPT process. However, the substitution of halogen atom affected the relative stability, $S_0 \rightarrow S_1$ adiabatic transition energy, structural parameter, and barrier height of nX7AI-H_2O during proton-transfer process. Our calculated results showed that the most stable complex of 7AI-H_2O derivatives is in the form of 6X7AI-H_2O (X = F, Cl, Br) in water. The transition energies in the nX7AI-H_2O (X = F, Cl, Br) complexes are linearly dependent on the Pauling electronegativity of halogen atom X. The halogen substitution increases/decreases the H-bond distances in the reactant, product, and structural parameters in the TS, which leads to enlarge the asynchronousity of proton transfer. The ESPT barrier height of nX7AI-H_2O is influenced by the halogen atom and substituted position. When the H atom at C_2, C_3 or C_4, and C_6 position is replaced by X, the ZPE-corrected barrier height reduces by 0.72~2.24 kcal/mol or increases by 0.34~2.44 kcal/mol. And the replacement of X at C_5 position makes the barrier height rise/reduce due to the substituent halogen atom X. The changes in the sum of N_1–O_{11} and O_{11}–N_7 distances have good correlations with Pauling electronegativity of halogen atom X.

Funding information This work was supported by grants from the National Natural Science Foundation of China (21403114), the Natural Science Foundation of Jiangsu province (BK20140970), and the Scientific Research Foundation for the Returned Overseas Chinese Scholars, State Education Ministry.

Compliance with ethical standards

We certify that this manuscript is original and has not been published and will not be submitted elsewhere for publication while being considered by Structural Chemistry. And the study is not split up into several parts to increase the quantity of submissions and submitted to various journals or to one journal over time. No data have been fabricated or manipulated (including images) to support your conclusions. No data, text, or theories by others are presented as if they were our own.

The submission has been received explicitly from all co-authors. And authors whose names appear on the submission have contributed sufficiently to the scientific work and therefore share collective responsibility and accountability for the results.

Conflict of interest The authors declare that they have no conflict of interest.

Human and animal studies This article does not contain any studies with human participants or animals performed by any of the authors.

Informed consent Informed consent was obtained from all individual participants included in the study.

Author agreement All authors have read and approved to submit it to your journal. There is no conflict of interest of any authors in relation to the submission. This paper has not been submitted elsewhere for consideration of publication.

References

1. Tuckerman ME, Marx D, Parrinello M (2002). Nature 417:925
2. Haw JF, Xu T, Nicholas JB, Goguen PW (1997). Nature 389:832
3. Blomberg MRA, Siegbahn PEM (2006). Biochim Biophys Acta 1757:969
4. Gutman M, Nachliel E (1997). Annu Rev Phys Chem 48:329
5. Mohammed OF, Pines D, Nibbering ETJ, Pines E (2006). Angew Chem Int Ed 46:1458
6. Chen K, Hirst J, Camba R, Bonagura CA, Stout CD, Burgess BK, Armstrong FA (2000). Nature 405:814
7. Lill MA, Helms V (2002). Proc Natl Acad Sci 99:2778
8. Wraight CA (2006). Biochem Biophys Acta 1757:886
9. Mathias G, Marx D (2007). Proc Natl Acad Sci 104:6980
10. Royant A, Edman K, Ursby T, Pebay-Peyroula E, Landau EM, Neutze R (2000). Nature 406:645
11. Faxén K, Gilderson G, Ädelroth P, Brzezinski P (2005). Nature 437: 286
12. Lu D, Voth GA (1998). J Am Chem Soc 102:4006
13. Kohen A, Cannio R, Bartolucci S, Klinman JP (1999). Nature 399:496
14. Pomés R, Roux B (2002). Biophys J 82:2304
15. Scheiner S (2000). J Phys Chem A 104:5898
16. Tolbert LM, Solntsev KM (2002). Acc Chem Res 35:19
17. Wu J, Liu W, Ge J, Zhang H, Wang P (2011). Chem Soc Rev 40:3483
18. Arnaut LG, Formosinho SJ (1993). J Photochem Photobiol A 75:1
19. Nir E, Kleinermanns K, de Vries MS (2000). Nature 408:949
20. Paddock ML, Feher G, Okamura MY (2003). FEBS Lett 555:45
21. Taylor CA, El-Bayoumi MA, Kasha M (1969). Proc Nat Acad Sci 63:253
22. Gordon MS (1996). J Phys Chem 100:3974
23. Nakajima A, Hirano M, Hasumi R, Kaya K, Watanabe H, Carter C, Williamson J, Miller TA (1997). J Phys Chem A 101:392
24. Chaban GM, Gordon MS (1999). J Phys Chem A 103:185
25. Fernández-Ramos A, Smedarchina Z, Siebrand W, Zgierski MZ (2001). J Chem Phys 114:7518
26. Yokoyama H, Watanabe H, Omi T, Ishiuchi S, Fujii M (2001). J Phys Chem A 105:9366
27. Casadesús R, Moreno M, Lluch JM (2003). Chem Phys 290:319
28. Kwon OH, Lee YS, Park HJ, Kim YH, Jang DJ (2004). Angew Chem Int Ed 43:5792
29. Taketsugu T, Yagi K, Gordon MS (2005). Int J Quantum Chem 104: 758
30. Hara A, Sakota K, Nakagaki M, Sekiya H (2005). Chem Phys Lett 407:30
31. Sakota K, Komoto Y, Nakagaki M, Ishikawa W, Sekiya H (2007). Chem Phys Lett 435:1
32. Sakota K, Inoue N, Komoto Y, Sekiya H (2007). J Phys Chem A 111:4596
33. Kina D, Nakayama A, Noro T, Taketsugu T, Gordon MS (2008). J Phys Chem A 112:9675
34. Koizumi Y, Jouvet C, Tsuji N, Ishiuchi S, Dedonder-Lardeux C, Fujii M (2008). J Chem Phys 129:104311
35. Sakota K, Komure N, Ishikawa W, Sekiya H (2009). J Chem Phys 130:224307
36. Duong MPT, Kim YH (2010). J Phys Chem A 114:3403
37. Sakota K, Jouvet C, Dedonder C, Fujii M, Sekiya H (2010). J Phys Chem A 114:11161
38. Fang H, Kim YH (2011). J Chem Theory Comput 7:642
39. Pino GA, Alata I, Dedonder C, Jouvet C, Sakota K, Sekiya H (2011). Phys Chem Chem Phys 13:6325
40. Fang H, Kim YH (2011). J Phys Chem A 115:13743
41. Daeungern R, Kungwan N, Woschann P, Aquino AJA, Lischka H, Barbatti M (2011). J Phys Chem A 115:14129
42. Yu XF, Yamazaki S, Taketsugu T (2011). J Chem Theory Comput 7:1006
43. Yu XF, Yamazaki S, Taketsugu T (2012). J Comput Chem 33:1701
44. Nakano H (1993). J Chem Phys 99:7983
45. Krygowski TM, Szatylowicz H, Zachara JE (2005). J Chem Inf Model 45:652
46. Chou PT, Yu WS, Wei CY, Cheng YM, Yang CY (2001). J Am Chem Soc 123:3599
47. Tseng HW, Liu JQ, Chen YA, Chao CM, Liu KM, Chen CL, Lin TC, Hung CH, Chou YL, Lin TC, Wang TL, Chou PT (2015). J Phys Chem Lett 6:1477
48. Chen YA, Meng FY, Hsu YH, Hung CH, Chen CL, Chung KY, Tang WF, Hung WY, Chou PT (2016). Chem Eur J 22:14688
49. Nazarparvar E, Zahedi M, Klein E (2012). J Org Chem 77:10093
50. Klein E, Lukeš V (2006). J Phys Chem A 110:12312
51. Solntsev KM, Poizat O, Dong J, Rehault J, Lou YB, Burda C, Tolbert LM (2008). J Phys Chem B 112:2700
52. Zhao Y, Truhlar DG (2008). Theor Chem Accounts 120:215
53. Frisch MJ, Truck GW, Schlegel HB, Scuseria GE, Robb MA, Cheeseman JR, Scalmani G, Barone V, Mennucci B, Petersson GA, Nakatsuji H, Caricato M, Li X, Hratchian HP, Izmaylov AF, Bloino J, Zheng G, Sonnenberg JL, Hada M, Ehara M, Toyota K, Fukuda R, Hasegawa J, Ishida M, Nakajima T, Honda Y, Kitao O, Nakai H, Vreven T, Montgomery Jr JA, Peralta JE, Ogliaro F, Bearpark M, Heyd JJ, Brothers E, Kudin KN, Staroverov VN, Kobayashi R, Normand J, Raghavachari K, Rendell A, Burant JC, Iyengar SS, Tomasi J, Cossi M, Rega N, Millam JM, Klene M, Knox JE, Cross JB, Bakken V, Adamo C, Jaramillo J, Gomperts R, Stratmann RE, Yazyev O, Austin AJ, Cammi R, Pomelli C, Ochterski JW, Martin RL, Morokuma K, Zakrzewski VG, Voth GA, Salvador P, Dannenberg JJ, Dapprich S, Daniels AD, Farkas O, Foresman JB, Ortiz JV, Cioslowski J, Fox DJ (2009) Gaussian 09. Gaussian Inc., Wallingford CT
54. Cances E, Mennucci B, Tomasi J (1997). J Chem Phys 107:3032
55. Cossi M, Barone V, Mennucci B, Tomasi J (1998). Chem Phys Lett 286:253

56. Mennucci B, Tomasi J (1997). J Chem Phys 106:5151
57. Glendening ED (2005). J Phys Chem A 109:11936
58. Glendening ED, Landis CR, Weinhold F (2013). J Comput Chem 35:1429
59. Weinhold F, Landis CR (2005) Valency and bonding: a natural bond orbital donor-acceptor perspective. University Press, Cambridge, Cambridge
60. Tanner C, Manca C, Leutwyler S (2003). Science 302:1736
61. Fang WH (1999). J Am Chem Soc 103:5567
62. Tanner C, Manca C, Leutwyler S (2005). J Chem Phys 122:204326
63. Ashfold MNR, Cronin B, Devine AL, Dixon RN, Nix MGD (2006). Science 312:1637
64. Yi JC, Fang H (2018). Photochem Photobiol 94:27
65. Mohammed OF, Pines D, Nibbering ETJ, Pines E (2007). Angew Chem Int Ed 46:1458
66. Brown ID (1992). Acta Cryst B 48:553
67. Limbach HH, Pietrzak M, Benedict H, Tolstoy PM, Golubev NS, Denisov GS (2004). J Mol Struct 706:115
68. Limbach HH, Lopez JM, Kohen A (2006). Philos Trans R Soc B 361:1399
69. Limbach HH (2007) In: Schowen RL, Klinman JP, Hynes JT, Limbach HH (eds) In hydrogen-transfer reactions. Wiley, Weinheim, Chapter 6, p 135221
70. Fang WH (1998). J Am Chem Soc 120:7568
71. Limbach HH, Schowen KB, Schowen RL (2010). J Phys Org Chem 23:586